

RESEARCH

Open Access



Development and validation of a novel vault prediction formula based on structural parameters of the anterior and posterior chambers

Wanmin Wu¹, Jiewei Liu¹, Long Zhang¹, Wenjie Liu¹, Ying Chang¹, Lichun Yang¹, Zeqi Fan¹, Bing Wang¹, Feiyan Chai¹, Jack X. Ma² and Junhong Li^{1*}

Abstract

Background Accurate prediction of postoperative vault in implantable collamer lens (ICL) implantation is crucial; however, current formulas often fail to account for individual anatomical variations, leading to suboptimal visual outcomes and necessitating improved predictive models. We aimed to verify the prediction accuracy of our new predictive model for vaulting based on anterior and posterior chamber structural parameters.

Methods This retrospective observational study included 137 patients (240 eyes) who previously underwent ICL surgery. Patients were randomly divided into the model establishment (192 eyes) or validation (48 eyes) groups. Preoperative measurements of the anterior and posterior chamber structures were obtained using Pentacam, CASIA2 anterior segment optical coherence tomography (AS-OCT), ultrasound biomicroscopy, and other devices. Stepwise multiple linear regression analysis was used to evaluate the relationship between the vault and each variable (WL formula). The Friedman test was performed for the vaulting prediction results of the WL, NK (Ver. 3), and KS formulas (Ver. 4) in CASIA2 AS-OCT, as well as the Zhu formula and vault measurements. The proportions of prediction error within $\pm 250 \mu\text{m}$ per formula were compared.

Results The predicted vault values of the WL, NK, KS, and Zhu formulas and vault measurements were 668.74 ± 162.12 , 650.85 ± 248.47 , 546.56 ± 128.99 , 486.56 ± 210.76 , and $716.06 \pm 233.84 \mu\text{m}$, respectively, with a significant difference ($\chi^2 = 69.883$, $P = 0.000$). Significant differences were also found between the measured vault value and Zhu formula, measured vault value and KS formula, WL formula and Zhu formula, WL formula and KS formula, NK formula and KS formula, and NK formula and Zhu formula ($P < 0.001$) but not between other groups. The proportions of prediction error within $\pm 250 \mu\text{m}$ per formula were as follows: WL formula (81.3%) > NK formula (70.8%) > KS formula (66.7%) > Zhu formula (54.2%).

Conclusions The WL formula, which considers the complexity of the anterior and posterior chamber structures, demonstrates greater calculation accuracy, compared with the KS (Ver. 4) and Zhu formulas. The proportion of

*Correspondence:

Junhong Li
junhongli2022@163.com

Full list of author information is available at the end of the article



© The Author(s) 2024. **Open Access** This article is licensed under a Creative Commons Attribution-NonCommercial-NoDerivatives 4.0 International License, which permits any non-commercial use, sharing, distribution and reproduction in any medium or format, as long as you give appropriate credit to the original author(s) and the source, provide a link to the Creative Commons licence, and indicate if you modified the licensed material. You do not have permission under this licence to share adapted material derived from this article or parts of it. The images or other third party material in this article are included in the article's Creative Commons licence, unless indicated otherwise in a credit line to the material. If material is not included in the article's Creative Commons licence and your intended use is not permitted by statutory regulation or exceeds the permitted use, you will need to obtain permission directly from the copyright holder. To view a copy of this licence, visit <http://creativecommons.org/licenses/by-nc-nd/4.0/>.

absolute prediction error $\leq 250 \mu\text{m}$ is higher with the WL formula than with the NK formula (ver. 3). This enhanced predictive capability can improve ICL sizing decisions, thereby increasing the safety and efficacy of ICL implantation surgeries.

Keywords Implantable collamer lens, Vault, Vault prediction formula, Pentacam, CASIA2 anterior segment optical coherence tomography, IOLMaster 700, Ultrasound biomicroscopy, Anterior chamber, Posterior chamber

Background

Recent research has indicated that the current global prevalence of myopia exceeds 22.9%, with projections suggesting a staggering increase to 49.8% by 2050. This surge in myopia encompasses approximately 938 million individuals with high myopia, accounting for about 9.8% of the global population [1]. Implantable collamer lens (ICL) implantation is a new and effective surgical method for treating ocular refractive errors, particularly high myopia. Compared with traditional corneal laser surgery, ICL has the advantages of safety, “reversibility,” high definition, little effect on dry eye, and wide correction range [2–6].

Although both ICL and intraocular lens (IOL) can be implanted into the eye and correct myopia, the lens material, design, location of implantation, calculation method, and surgical method are different [7, 8]. ICL uses collamer material, and the front of the lens is a plate composed of the optical part and the four haptics; however, the optical part and the four haptics are not climbing on the same plane; the side is arched so that the ICL can be supported in the ciliary sulcus. The operation is ICL implantation, which does not damage the natural lens, and the eye still retains the accommodation of the natural lens after the operation. The parameters used for ICL calculation include refraction, corneal curvature, anterior chamber depth, corneal thickness, and white-to-white (WTW) corneal diameter. The ICL power and size are calculated by a special network calculator provided by STAAR Surgical Company [9].

In contrast, the acrylic material of the IOL is more rigid, compared with the collamer. The shape of the IOL can be flat; the four haptics of the flat style are basically on the same plane with the optical part so that the IOL can be supported in the lens capsule. The parameters used for IOL calculation include corneal curvature, axial length, anterior chamber depth, corneal thickness, lens thickness, and WTW, which can be calculated using Barrett Universal II, Kane, PEARL-DGS, or other formulas [10].

The surgical technique for ICL implantation has been used worldwide for nearly 30 years and for over 15 years in China. Over 1 million ICLs have been implanted in the eyes of patients worldwide. With the increased use of ICL, ensuring vault safety has become a major concern in clinical practice. The vault refers to the vertical distance between the center of the posterior surface of the ICL

lens and the anterior apex of the natural lens [11]. Ensuring the achievement of an ideal vault after ICL surgery is crucial for determining its safety. When the vault of an implanted ICL is too high, iris extrusion can occur and lead to the narrowing or closure of the chamber angle, resulting in angle-closure glaucoma. Additionally, a high vault may increase the risk of pigment-disseminated glaucoma, iris atrophy, and postoperative anterior chamber inflammation owing to the close contact between the ICL and the posterior surface of the iris [12]. Conversely, a low vault can result in excessive proximity or contact between the ICL and natural lens, thereby increasing the risk of mechanical friction between the ICL and the natural anterior capsule of the lens. This impedes aqueous humor circulation and ultimately affects the metabolism of lens epithelial cells, leading to the development of anterior subcapsular cataract [13]. Previous research has suggested that the ideal vault range should be controlled between $250 \mu\text{m}$ and $750 \mu\text{m}$ [14]. However, the nomogram provided by the ICL lens manufacturer (STAAR Surgical) alone cannot ensure that an appropriate ICL size is implanted for every patient. One study showed that only 50.5% of the ICL size was ideal after surgery when the manufacturer’s nomogram was used to calculate the ICL size [15] because the manufacturer’s nomogram only used the WTW distance and the internal anterior chamber depth (iACD) (i.e., the distance from the central corneal endothelium to the native crystal). However, these two parameters do not explain the complexity of the intraocular structure. Many variations in the structure of the ciliary sulcus exist in the posterior chamber of the eye where the ICL is placed. Studies have shown that horizontal ciliary sulcus to ciliary sulcus (hSTS), vertical ciliary sulcus to ciliary sulcus (vertical sulcus to ciliary sulcus [vSTS]), distance between the hSTS plane and anterior crystalline lens surface (hSTSL), crystalline lens rise (CLR), lens thickness (LT), and other posterior chamber structural parameters are correlated with the vault [9, 16].

To date, no “gold standard” formula for predicting the vault of ICL has been developed. Accurately predicting the vault after ICL implantation and optimizing the size of the ICL are challenges in the design of ICL implantation surgery and problems that need to be solved urgently in clinical diagnosis and treatment. In this study, the Pentacam, CASIA2 anterior segment optical coherence tomography (AS-OCT), IOLMaster 700, ultrasound

biomicroscopy (UBM), and other measuring devices were used to accurately and comprehensively measure the anterior and posterior chamber structures before surgery. The factors affecting the vault were comprehensively analyzed to explore the influence of anterior and posterior chamber structural parameters on the vault. A multiple linear regression equation was used to establish the prediction model of the vault 1 month after surgery. This study aimed to validate the accuracy of the vaulting prediction model and compare it with the NK formula (Ver. 3) and KS formula (Ver. 4) embedded in CASIA2 AS-OCT and the Zhu formula published by Zhu et al. [17], while considering the anterior and posterior chamber structures. Finally, we proposed an improved surgical design for ICL implantation to enhance the predictability and safety of surgical outcomes.

Methods

Study population

Clinical data of 137 patients (240 eyes) with myopia who underwent V4c ICL (STAAR Surgical Co.) implantation in our hospital from July 2023 to May 2024 were collected. The patients were randomly divided into the model establishment or validation groups, which consisted of 192 and 48 eyes, respectively. The inclusion criteria were as follows: (1) anterior chamber depth ≥ 2.8 mm, open chamber angle, corneal endothelial cell count $\geq 2,000$ /mm², and stable cell morphology; (2) no other ocular diseases that could significantly affect visual acuity or systemic organic lesions that could affect surgical recovery; and (3) patients' surgical eyes undergoing monocular surgery were considered the research objects (if one eye of a patient who underwent bilateral surgery met the exclusion criteria or was excluded from the study, and the contralateral eye met the inclusion criteria, the contralateral eye was selected as the study object; if both eyes met the inclusion criteria, both were included in the study); and (4) the non-astigmatism ICL was placed horizontally, whereas the toric ICL was implanted at $\leq 10^\circ$ rotation, compared with the horizontal position. The exclusion criteria were as follows: iris-ciliary body cysts, glaucoma, uveitis, active eye disease or infection, or other eye diseases; failure to return to the hospital on time; incomplete postoperative examination data; and replacement of the ICL size during follow-up.

Our study protocol adhered to the principles outlined in the Declaration of Helsinki established by the World Medical Association. It mandated that all participants receive comprehensive information regarding the study's objectives and associated risks and provide their written informed consent by signing a surgical consent form. The present study was granted ethical approval by the Ophthalmology Ethical Committee of Shanxi Province, with the reference number SXYYLL-20,210,601.

Preoperative examination

All patients with complete clinical data, including sex, age, and other relevant information, were included in this study. Prior to surgery, the patients underwent comprehensive ophthalmic examinations, including subjective refraction assessment, non-contact tonometry for intraocular pressure measurement, corneal endothelial cell density evaluation, slit-lamp microscopy, and routine fundus examination, which were converted to a spherical equivalent (SE). Special examinations included anterior segment panoramic analysis (Pentacam; Oculus; Germany), AS-OCT (CASIA2 AS-OCT; Tomey; Nagoya, Japan), biometer (IOLMaster 700; Carl Zeiss Meditec AG; Jena, Germany), and UBM (SW-3200 L; SUOER; Tianjin, China). Pentacam inspection included iACD, steep keratometry (K_s), flat keratometry (K_f), central corneal thickness (CCT), WTW, anterior chamber volume (ACV), and anterior chamber angle (ACA). CASIA2 AS-OCT was performed as described by Wu et al. [18]. The examination included anterior chamber width (ACW), CLR, bilateral angle-to-angle (ATA), and results of vault prediction using the NK (Ver. 3) and KS formulas (Ver. 4). The axial length (AL) and LT were measured using IOLMaster 700.

The UBM examination method was performed as described in the study by Zhang et al. [19], and the measurement parameters included posterior chamber angle at 3, 6, 9, and 12 o'clock (PCA_{3,6,9,12}); width of the ciliary sulcus recess at 3, 6, 9, and 12 o'clock (CSR_{3,6,9,12}); linear distance from posterior surface of peripheral iris to ciliary processes at 3, 6, 9, and 12 o'clock (LD-ITC_{3,6,9,12}); height of ciliary processes at 3, 6, 9, and 12 o'clock (HCP_{3,6,9,12}); hSTS; vSTS; hSTSL; and distance between the vSTS plane and anterior crystalline lens surface (vSTSL) (Fig. 1).

Surgical technique and postoperative follow-up

Based on the subjective refraction and measurement results of the Pentacam, the STAAR calculator network provided by the company was used to calculate the preimplanted ICL power and size. The pupil was fully dilated with compound tropicamide eye drops 30 min before the operation, and topical anesthesia was preoperatively administered with proparacaine hydrochloride eye drops. The ICL chamber was hydrated with balanced salt solution under the operating microscope, and the ICL was preloaded for use. The ICL was carefully inserted into the anterior chamber while ensuring stability to prevent any potential rotation. An appropriate amount of viscoelastic agent was injected in front of the ICL, and the four haptics of the ICL were carefully positioned within the ciliary sulcus posterior to the iris using an adjustment hook. The viscoelastic agent was completely removed from the anterior chamber balanced salt solution, and the incision

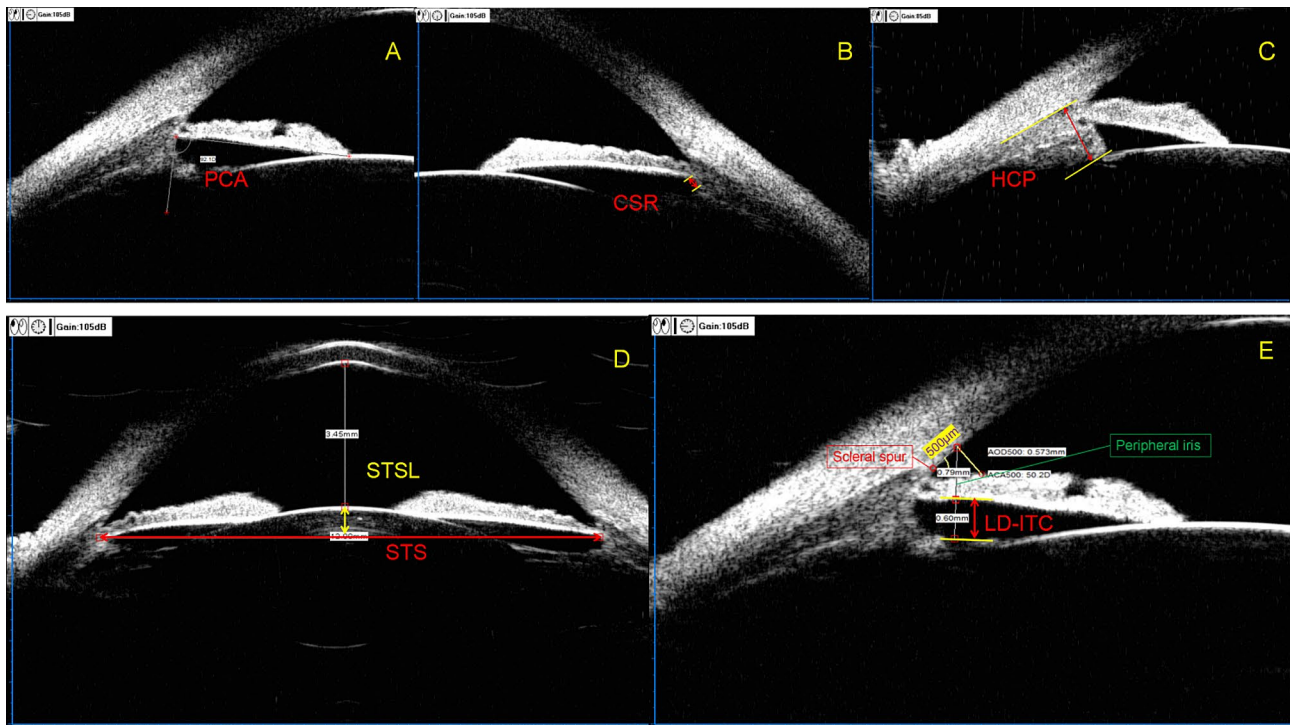


Fig. 1 Measurement parameters of UBM. **(a)** PCA, posterior chamber angle=the angle formed between the posterior surface of the iris root and the anterior aspect of the ciliary body. **(b)** CSR, width of the ciliary sulcus recess=the width of the recess formed on the posterior surface of the iris root and the anterior portion of the ciliary body. **(c)** HCP, height of ciliary processes=the distance from the tip to the base of the ciliary processes. **(d)** STS, ciliary sulcus to ciliary sulcus=inter-ciliary sulcal distance within the same meridional orientation; STSL, distance between the STS plane and anterior crystalline lens surface. **(e)** LD-ITC, linear distance from the posterior surface of the peripheral iris to the ciliary processes. Peripheral iris refers to the portion of the iris located 500 μm above the scleral spur along the corneal endothelium, measured as a straight line perpendicular to the anterior surface of the iris

was made watertight to maintain moderate intraocular pressure. All operations were performed by a single surgeon using the same surgical method, and the ICL was implanted in the ciliary sulcus. The surgeries were performed successfully with no ICL implantation-related complications. The patients were followed up at 1 day, 1 week, and 1 month postoperatively, with subsequent recording of vault measurements using CASIA2 AS-OCT performed at the 1-month follow-up visit.

Model establishment, model validation, and parameter calculation

Model establishment

Taking SE, iACD, WTW, ACV, ACA, K_p , K_s , CCT, ACW, CLR, ATA, AL, LT, $PCA_{3,6,9,12}$, $HCP_{3,6,9,12}$, $CSR_{3,6,9,12}$, LD-ITC_{3,6,9,12}, hSTS, vSTS, hSTSL, vSTSL, and ICL size as independent variables and vault at 1 month postoperatively as the dependent variable, a multiple linear regression equation, that is, the WL formula (short for Wu-Liu formula), was established.}

Model validation

Validation group data were separately integrated into the WL formula, and the Zhu formula [17] (central vault [μm] = $-1369.05 + 657.121 \times \text{ICL size} - 287.408 \times \text{hSTS}$

$432.497 \times \text{LT}137.33 \times \text{vSTS}$) was calculated and combined with the NK and KS formula of CASIA2 AS-OCT.

Calculation of parameters

Calculated parameters included the following: prediction error (PE) (PE=measured value of vault at 1 month postoperatively minus predicted value of vault calculation formula); mean prediction error; absolute prediction error (APE) (APE=|PE|); mean absolute error; and median of absolute error (MedAE).

Statistical analysis

The recorded measurement data underwent a normality test. Measurement data exhibiting normal distributions were presented as means \pm standard deviations, and those exhibiting non-normal distributions were represented as medians (interquartile ranges). An independent samples t-test was employed to compare the ocular structural parameters between the groups for model establishment and validation. The statistical significance of multiple linear regression equations was assessed using analysis of variance. The coefficient of determination (R^2) was used to evaluate the model's goodness of fit. The Durbin-Watson test was employed to assess the independence of the residuals, while the variance inflation factor (VIF) was

Table 1 Baseline characteristics of the study patients (240 eyes)

Characteristic	Mean ± SD	Range
Age, years	27.56 ± 6.16	18 to 50
Sex (male/female)	17/120	
SE (D)	-9.64 ± 2.94	-20.25 to -2.50
Pentacam		
iACD (mm)	3.22 ± 0.24	2.70 to 3.91
WTW (mm)	11.53 ± 0.37	10.60 to 12.60
ACV (mm ³)	191.15 ± 30.07	133 to 289
ACA (°)	38.63 ± 4.62	28.00 to 50.40
K _f (D)	43.14 ± 1.45	38.70 to 46.80
K _s (D)	44.87 ± 1.74	39.20 to 49.20
CCT (μm)	526.06 ± 29.30	456 to 607
IOLMaster 700		
AL (mm)	26.84 ± 1.38	23.79 to 31.16
LT (mm)	3.68 ± 0.24	3.20 to 4.44
UBM		
hSTS (mm)	11.36 ± 0.48	10.07 to 12.79
vSTS (mm)	11.80 ± 0.49	10.37 to 13.92
hSTSL (mm)	0.28 ± 0.19	-0.02 to 0.92
vSTSL (mm)	0.44 ± 0.18	0 to 1.03
PCA ₃ (°)	64.37 ± 32.77	0 to 136.40
CSR ₃ (mm)	0.11 ± 0.18	0 to 0.70
LD-ITC ₃ (mm)	0.41 ± 0.20	0 to 0.88
HCP ₃ (mm)	1.31 ± 0.15	0.63 to 1.63
PCA ₉ (°)	65.38 ± 32.38	0 to 138.80
CSR ₉ (mm)	0.11 ± 0.18	0 to 0.70
LD-ITC ₉ (mm)	0.42 ± 0.18	0 to 0.98
HCP ₉ (mm)	1.35 ± 0.15	0.85 to 1.74
PCA ₆ (°)	67.16 ± 34.33	0 to 145.20
CSR ₆ (mm)	0.12 ± 0.19	0 to 0.98
LD-ITC ₆ (mm)	0.40 ± 0.18	0 to 0.98
HCP ₆ (mm)	1.32 ± 0.15	0.74 to 1.87
PCA ₁₂ (°)	86.48 ± 33.78	0 to 146.00
CSR ₁₂ (mm)	0.22 ± 0.21	0 to 0.78
LD-ITC ₁₂ (mm)	0.53 ± 0.19	0 to 1.00
HCP ₁₂ (mm)	1.29 ± 0.15	0.72 to 1.72
CASIA2 AS-OCT		
ACW (mm)	11.57 ± 0.35	10.52 to 12.52
CLR (mm)	31.83 ± 177.57	-649 to 460
ATA (mm)	11.69 ± 0.36	10.67 to 12.69
ICL size (12.1/12.6/13.2/13.7)	37/142/55/6	
Vault (1 month) (μm)	683.42 ± 211.63	144 to 1440

SE, spherical equivalent; iACD, internal anterior chamber depth; WTW, white-to-white; ACV, anterior chamber volume; ACA, anterior chamber angle; K_f, flat keratometry; K_s, steep keratometry; CCT, central corneal thickness; AL, axial length; LT, lens thickness; hSTS, horizontal ciliary sulcus to ciliary sulcus; vSTS, horizontal ciliary sulcus to ciliary sulcus; hSTSL, distance between hSTS plane and anterior crystalline lens surface; vSTSL, distance between vSTS plane and anterior crystalline lens surface; PCA_{3,6,9,12}, posterior chamber angle at 3, 6, 9, 12 o'clock; CSR_{3,6,9,12}, width of the ciliary sulcus recess at 3, 6, 9, 12 o'clock; LD-ITC, linear distance from posterior surface of peripheral iris to ciliary process; HCP, height of ciliary processes; ACW, anterior chamber width; CLR, crystalline lens rise; ATA, angle-to-angle; ICL size, implantable collamer lens size (STAAR Surgical)

used to examine potential multicollinearity among the independent variables in the model. The Friedman test was employed to compare the computed results of the WL, NK, KS, and Zhu formulas with the measured values of vaulting in the model validation group. The Friedman test was conducted on the APE of each formula, and the Nemenyi post-hoc test was employed for inter-group comparisons. Statistical significance was defined as $P < 0.05$. The P -values were calculated using standard statistical software (SPSS v25.0, IBM Corp., Armonk, NY, USA).

Results

The detailed demographic and clinical characteristics of the participants are presented in Table 1. A total of 240 eyes from 137 patients (17 male and 120 female participants) with an average age of 27.56 ± 6.16 years, ranging from 18 to 50 years, were included in the study. The average ICL size was 12.68 ± 0.38 mm, including 37 eyes with a size of 12.1 mm, 142 eyes with a size of 12.6 mm, 55 eyes with a size of 13.2 mm, and 6 eyes with a size of 13.7 mm. The model establishment and validation groups demonstrated significant disparities in PCA₃ and CSR₃ ($P = 0.014$ and $P = 0.003$, respectively). No significant differences were observed in other parameters between the two groups (Table 2).

Model establishment

The results of the multiple linear regression analysis revealed a positive correlation with 1-month vault and ICL size, whereas negative correlations were observed with CCT, ATA, hSTSL, vSTSL, CSR₃, LD-ITC₆, and LD-ITC₉. The WL formula was as follows: Vault = $-587.182 + 396.551 \times \text{ICL size} + 1.085 \times \text{CCT} + 242.064 \times \text{ATA} + 236.778 \times \text{hSTSL} + 258.846 \times \text{vSTSL} + 154.281 \times \text{CSR}_3 + 207.966 \times \text{LD-ITC}_9 + 218.537 \times \text{LD-ITC}_6$ ($R = 0.702$, $R^2 = 0.492$, adjusted $R^2 = 0.470$). The results of the Durbin–Watson test revealed that $U = 1.837$, close to 2, proving the parameters of independence. The VIF of each parameter in the equation were < 5 , and eight parameters did not exhibit multicollinearity. The fitting model of variance analysis showed that $F = 22.055$ and $P = 0.000$, and the model after inspection within the respective variables revealed all $P < 0.05$, suggesting that the fitting model and the model for all variables were significant (Table 3).

Model validation

The predicted vault values of the WL, NK, KS, and Zhu formulas and measured vault value were 668.74 ± 162.12 , 650.85 ± 248.47 , 546.56 ± 128.99 , 486.56 ± 210.76 , and 716.06 ± 233.84 μm, respectively. The Friedman test showed that $c^2 = 69.883$ and $P = 0.000$, and the difference was significant. The Nemenyi test on the comparisons

Table 2 Baseline characteristics of the model establishment and model validation groups

Characteristic	Model establishment group	Model validation group	P-value
Number of eyes	192	48	
Age, years	27.54 ± 6.24	27.38 ± 5.64	0.666
Sex (male/female)	17/113	5/42	0.881
SE (D)	-9.62 ± 3.03	9.76 ± 2.54	0.763
Pentacam			
iACD (mm)	3.22 ± 0.25	3.21 ± 0.23	0.702
WTW (mm)	11.52 ± 0.37	11.60 ± 0.36	0.177
ACV (mm ³)	190.91 ± 30.14	192.08 ± 30.07	0.810
ACA (°)	38.76 ± 4.71	38.11 ± 4.23	0.380
K _f (D)	43.15 ± 1.47	43.06 ± 1.38	0.689
K _s (D)	44.89 ± 1.77	44.81 ± 1.62	0.764
CCTS (microns)	526.39 ± 29.50	524.77 ± 28.75	0.734
IOLMaster 700			
AL (mm)	26.85 ± 1.44	26.82 ± 1.13	0.880
LT (mm)	3.68 ± 0.23	3.70 ± 0.26	0.661
UBM			
hSTS (mm)	11.35 ± 0.48	11.37 ± 0.47	0.765
vSTS (mm)	11.81 ± 0.49	11.75 ± 0.48	0.448
hSTSL (mm)	0.27 ± 0.19	0.32 ± 0.18	0.088
vSTSL (mm)	0.43 ± 0.18	0.45 ± 0.17	0.471
PCA ₃ (°)	67.05 ± 33.68	55.46 ± 27.05	0.014 *
CSR ₃ (mm)	0.12 ± 0.18	0.05 ± 0.13	0.003 **
LD-ITC ₃ (mm)	0.41 ± 0.20	0.40 ± 0.17	0.648
HCP ₃ (mm)	1.31 ± 0.15	1.30 ± 0.16	0.915
PCA ₉ (°)	65.98 ± 31.95	63.02 ± 33.81	0.571
CSR ₉ (mm)	0.12 ± 0.19	0.09 ± 0.15	0.329
LD-ITC ₉ (mm)	0.43 ± 0.18	0.38 ± 0.18	0.077
HCP ₉ (mm)	1.35 ± 0.16	1.35 ± 0.14	0.923
PCA ₆ (°)	67.97 ± 34.74	63.93 ± 32.75	0.467
CSR ₆ (mm)	0.13 ± 0.19	0.11 ± 0.17	0.516
LD-ITC ₆ (mm)	0.40 ± 0.18	0.41 ± 0.19	0.658
HCP ₆ (mm)	1.32 ± 0.15	1.31 ± 0.12	0.642
PCA ₁₂ (°)	85.39 ± 35.00	90.82 ± 28.32	0.262
CSR ₁₂ (mm)	0.22 ± 0.21	0.25 ± 0.19	0.375
LD-ITC ₁₂ (mm)	0.53 ± 0.19	0.54 ± 0.19	0.668
HCP ₁₂ (mm)	1.29 ± 0.16	1.28 ± 0.15	0.675
CASIA2 AS-OCT			
ACW (mm)	11.56 ± 0.36	11.60 ± 0.34	0.485
CLR (mm)	41.70 ± 177.33	7.69 ± 174.79	0.085
ATA (mm)	11.68 ± 0.36	11.72 ± 0.34	0.566
ICL size (12.1/12.6/13.2/13.7)			
Vault (1 month) (μm)	675.26 ± 218.34	716.06 ± 233.84	0.255

* $P < 0.05$; ** $P < 0.001$; SE, spherical equivalent; iACD, internal anterior chamber depth; WTW, white-to-white; ACV, anterior chamber volume; ACA, anterior chamber angle; K_f, flat keratometry; K_s, steep keratometry; CCT, central corneal thickness; AL, axial length; LT, lens thickness; hSTS, horizontal ciliary sulcus to ciliary sulcus; vSTS, horizontal ciliary sulcus to ciliary sulcus; hSTSL, distance between hSTS plane and anterior crystalline lens surface; vSTSL, distance between vSTS plane and anterior crystalline lens surface; PCA_{3,6,9,12}, posterior chamber angle at 3, 6, 9, and 12 o'clock; CSR_{3,6,9,12}, width of the ciliary sulcus recess at 3, 6, 9, and 12 o'clock; LD-ITC_{3,6,9,12}, linear short from posterior surface of peripheral iris to ciliary process at 3, 6, 9, and 12 o'clock; HCP_{3,6,9,12}, height of ciliary the processes at 3, 6, 9, and 12 o'clock; ACW, anterior chamber width; CLR, crystalline lens rise; ATA, angle-to-angle; ICL size, implantable collamer lens size (STAAR Surgical)

between the vault measured value and Zhu formula, vault measured value and KS formula, WL formula and Zhu formula, WL formula and KS formula, NK formula and KS formula, and NK formula and Zhu formula indicated that the differences were significant ($P < 0.001$); however, there were no significant differences among the remaining comparisons (Fig. 2).

The APE values of the WL, NK, KS, and Zhu formulas were 156.27 ± 95.78 , 177.21 ± 120.31 , 204.83 ± 137.20 , and 261.09 ± 180.84 μm, respectively. The Friedman test showed $c^2 = 17.275$ and $P = 0.001$, and the difference was significant. The Nemenyi test on the comparisons of the WL formula and Zhu formula and WL formula and KS formula showed significant differences ($P = 0.001$ and $P = 0.029$, respectively); however, there were no significant differences among the remaining comparisons. MedAE comparisons of the formulas were as follows: WL formula (156.25 μm) < NK formula (170.50 μm) < KS formula (182.00 μm) < Zhu formula (215.47 μm). Comparisons of the proportions of PE within ± 250 μm of the formulas were as follows: WL formula (81.3%) > NK formula (70.8%) > KS formula (66.7%) > Zhu formula (54.2%) (Table 4). Figure 3 further shows that the proportion of PEs within ± 250 μm of the WL formula was higher than that of other prediction formulas. Figure 4 shows the APE changes of the four formulas under different ICL sizes (13.7 mm ICL size; only one eye's data were not included in this analysis). The four formulas exhibited the smallest disparity in APE prediction when the ICL size was 13.2 mm, whereas the discrepancy in APE prediction was the highest with an ICL size of 12.1 mm. With respect to vaulting prediction for a 12.1-mm ICL size, both the WL formula and KS formula demonstrated lower APE values, compared with the NK formula. However, the Zhu formula did not yield satisfactory accuracy in predicting vaulting for all three ICL sizes.

Discussion

In this study, we explored the influence of several parameters, including age, SE, iACD, WTW, ACV, ACA, K_f, K_s, CCT, ACW, CLR, ATA, AL, LT, PCA_{3,6,9,12}, HCP_{3,6,9,12}, CSR_{3,6,9,12}, LD-ITC_{3,6,9,12}, hSTS, vSTS, hSTSL, and vSTSL, on vaulting. Furthermore, ICL size, CCT, ATA, hSTSL, vSTSL, CSR₃, LD-ITC₆, and LD-ITC₉ were included in the regression equation, and a new multiple linear regression model, the WL formula, was established to predict the vault after ICL implantation. To verify the accuracy of the WL formula, this study used a new data model validation group with 48 eyes to calculate the WL formula and compared the calculated results with the published NK, KS, and Zhu formulas. The results showed that the WL formula prediction model had a relatively accurate prediction effect on vaulting in the first month after ICL surgery. This study creatively joined the 3, 6, 9,

Table 3 Multivariate analysis between the 1-month ICL vault and other parameters (constant = 587.182; $R=0.702$; $R^2=0.492$; adjusted $R^2=0.470$; Durbin–Watson (U) = 1.837; $F=22.055$, $P=0.000$)

Parameter	Partial regression coefficient (B)	Standardized partial regression coefficient (beta)	t	P-value	VIF
CCT	1.085	0.147	2.749	0.007 **	1.022
ATA	242.064	0.400	4.970	0.000 **	2.324
hSTSL	236.778	0.201	2.154	0.033 *	3.135
vSTSL	258.846	0.213	2.307	0.022 *	3.069
CSR ₃	154.281	0.128	2.200	0.029 *	1.218
LD-ITC ₉	207.966	0.176	2.841	0.005 **	1.373
LD-ITC ₆	218.537	0.180	2.803	0.006 **	1.476
ICL size	396.551	0.695	8.442	0.000 **	2.431

* $P<0.05$; ** $P<0.001$; CCT, central corneal thickness; ATA, angle-to-angle; hSTSL, distance between horizontal ciliary sulcus to ciliary sulcus plane and anterior crystalline lens surface; vSTSL, distance between horizontal ciliary sulcus to ciliary sulcus plane and anterior crystalline lens surface; CSR₃, posterior chamber angle at 3 o'clock; LD-ITC_{6,9}, linear short from posterior surface of peripheral iris to ciliary process at 6 and 9 o'clock; ICL size, implantable collamer lens size (STAAR Company); VIF, variance inflation factor

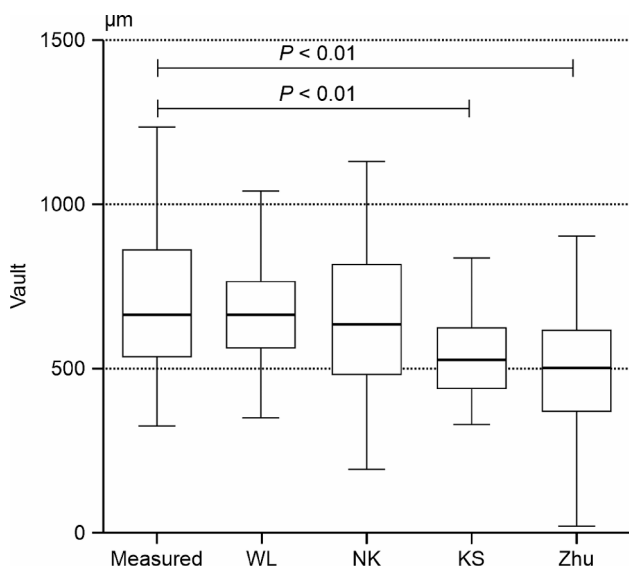


Fig. 2 Box plot comparing the measured vault and predicted vault for each formula Measured, vault measured in 1 month; WL, WL formula; NK, NK formula; KS, KS formula; Zhu, Zhu formula

and 12 points of PCA, HCP, CSR, and LD-ITC eye posterior chamber structure parameters; it incorporated a more comprehensive range of posterior chamber structure parameter, compared with previous studies. Our aim was to build a new multivariate linear regression model, that is, the WL formula, to choose ICL size and postoperative vault prediction for new support options. Further, our approach improves the safety of ICL implantation,

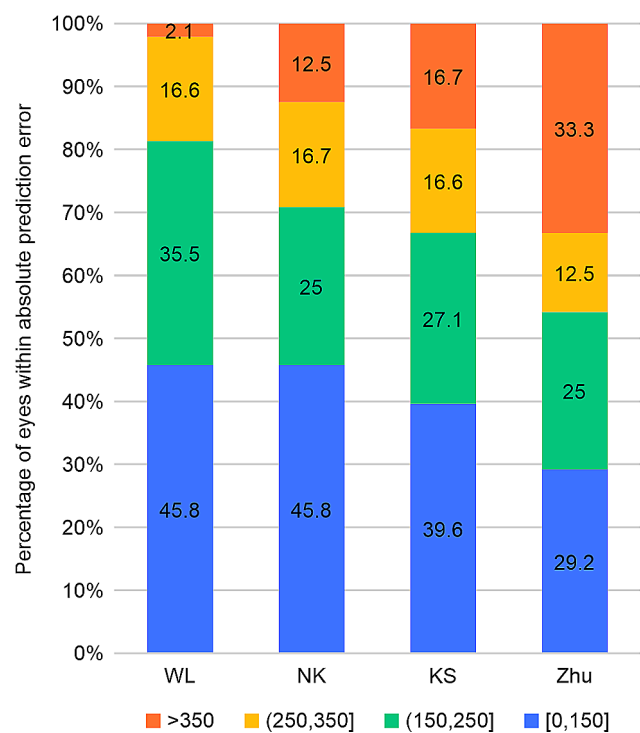


Fig. 3 Stacked histogram comparing the percentage absolute prediction error for each formula. WL, WL formula; NK, NK formula; KS, KS formula; Zhu, Zhu formula

and the parameters used in the formula do not need to be obtained using special equipment, which is conducive

Table 4 Vault prediction errors of each formula (model validation group, 48 eyes)

Formula	Percentage of eyes within indicated micrometer range				Percentage of eyes within indicated micrometer range		
	MAE (µm)	SD	MedAE (µm)	Quartile range (µm)	± 150 µm	± 250 µm	± 350 µm
WL	156.27	95.78	156.25	[74.82, 229.29]	45.8%	81.3%	97.9%
NK	177.21	120.31	170.50	[71.25, 267.50]	45.8%	70.8%	87.5%
KS	204.83	137.20	182.00	[88.25, 311.00]	39.6%	66.7%	83.3%
Zhu	261.09	180.84	215.47	[126.65, 442.72]	29.2%	54.2%	66.7%

WL, WL formula; NK, NK formula; KS, KS formula; Zhu, Zhu formula; MAE, mean absolute error; MedAE, median absolute error

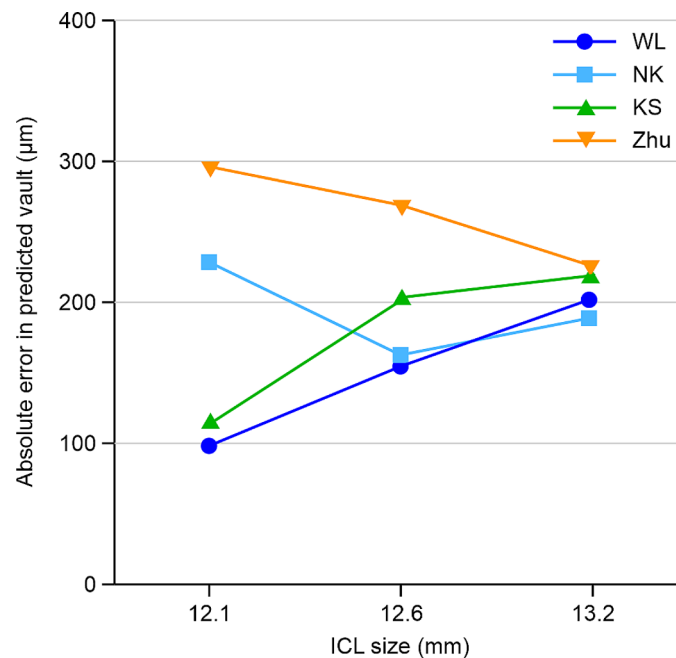


Fig. 4 Line graph of absolute error. The values for the four vault prediction formulas versus those for implantable collamer lens (STAAR Surgical) size is shown. WL, WL formula; NK, NK formula; KS, KS formula; Zhu, Zhu formula

to the clinical promotion and verification of the WL formula.

This study showed that the ATA, CCT, and vault anterior chamber structural parameters were negatively correlated with the vault. Many scholars have explored the relationship between the structural parameters of the anterior chamber and vault. Oleszko et al. [20] used a partial least squares regression algorithm to analyze the vault, ATA, ACD, and other parameters in 43 patients (81 eyes). The results showed that ATA was negatively correlated with postoperative vault, accounting for 16.1% of the effect on the vault. Trancón et al. [21] studied the clinical data of 360 eyes of 360 patients with myopia, and multiple linear regression showed that the standard regression coefficient (β) of ATA was -0.42 , indicating a negative correlation with postoperative vault. Kim et al. [22] conducted a regression model analysis of the ocular measurement data of 368 patients (696 eyes) based on the ANTERION biometer and postoperative vault measurement results. The results showed that the unstandardized coefficient of CCT was -0.33 ($P=0.026$), which was consistent with the results of the present study. ATA and CCT were negatively correlated with the vault possibly because, under the premise of the same ICL implant size, a wider ATA reduces the support of ICL haptics, thereby reducing the ICL vault. A previous study [23] has shown that iACD is positively correlated with vaulting; therefore, a thicker CCT may reduce iACD and lead to a lower vault.

Given that the ICL is eventually implanted in the ciliary sulcus of the posterior chamber of the eye, this study innovatively uses a total of 16 quantitative indicators, including $PCA_{3,6,9,12}$, $HCP_{3,6,9,12}$, $CSR_{3,6,9,12}$, and $LD-ITC_{3,6,9,12}$ based on the research of Wei et al. [24]. It also integrates the hSTS, vSTS, hSTSL, and vSTSL found in previous studies [25, 26] to comprehensively explore the influence of the differences in the posterior chamber structure on the vault. The results showed that the posterior chamber structural components hSTSL, vSTSL, CSR_3 , $LD-ITC_6$, and $LD-ITC_9$ were negatively correlated with vaulting, consistent with the results of Zou et al. [27]. However, previous studies have failed to quantitatively study the ciliary sulcus structure at four points in the horizontal and vertical directions. The negative correlation between hSTSL, vSTSL, CSR_3 , $LD-ITC_6$, and $LD-ITC_9$ and vaulting may be attributed to the size of the implanted ICL being unchanged; thus, a wider CSR and LD-ITC would reduce the support of the ICL haptics, resulting in an ICL crystal close to the natural lens and a decrease in the vault. Higher hSTSL and vSTSL values indicate that the protrusion of the natural crystal is obvious and that some of the natural crystal thickness occupies the space of the vault, which leads to a decrease in the vault measurement value.

A further study of the WL formula vaulting prediction model found that, with respect to individual factors, ICL size and ATA had the greatest impact on vaulting prediction (standardized partial regression coefficient (β), 0.695 and -0.400 , respectively), consistent

with the results of Igarashi et al. [28]. Standardized partial regression showed that the combined effect of the overall posterior chamber structural parameters ($hSTSL+vSTSL+CSR_3+LD-ITC_9+LD-ITC_6$) on vault prediction was higher than that of the overall anterior chamber structural parameters (ATA+CCT) (coefficient (β), 0.898 vs. 0.547), indicating that the selection of implanted ICL size should not only consider changes in anterior chamber structure, such as ATA and CCT but should also consider the abnormalities of posterior chamber structural parameters to achieve the ideal vault after ICL implantation.

This study aimed to validate the fitting model and compare it with the NK, KS, and Zhu formulas to verify the accuracy of the WL formula. The findings revealed that the WL formula had superior accuracy, compared with both the KS and Zhu formulas. In addition, the PE of the WL formula was within $\pm 250 \mu\text{m}$ and accounted for 81.3%, superior to that of other vaulting prediction formulas. Notably, this study has focused on the comparison of the proportion of PEs within the range of $\pm 250 \mu\text{m}$ because the ideal vault of ICL is generally $500 \mu\text{m}$, and the ideal vault range is $500 \pm 250 \mu\text{m}$ [14]. In clinical practice, to achieve an ideal vault after surgery, the predicted vault value of the calculation formula is set to $500 \mu\text{m}$. Then, the size of ICL to be implanted is calculated; thus, the postoperative PE within the range of $\pm 250 \mu\text{m}$ still falls within the ideal vault, which is within the medically acceptable range. The above results may be attributed to the fact that the WL formula model used a relatively large sample size of 192 eyes and was based on more parameters of the anterior and posterior chamber structure (34 parameters); therefore, the equation has a more comprehensive explanation for postoperative vault. The NK formula was obtained by Nakamura et al. [29], who measured the ocular data of 41 patients (81 eyes) and performed a regression analysis. This equation considers three parameters: the ACW, CLR, and ICL size. Igarashi et al. [28] used CASIA2 AS-OCT to measure the ocular parameters of 23 patients (44 eyes) and performed regression analysis to obtain the KS formula, which only had two variables: ICL size and ATA. The sample sizes of the NK and KS formulas were limited, and the analyses and calculations were only based on AS-OCT, without the use of UBM to explore the posterior chamber structure of the eye; therefore, the interpretations of the vault were limited. Zhu et al. [17] studied the ocular data of 83 patients (83 eyes). Although multiple anterior and posterior chamber structural parameters were considered in their study, the regression equation only included four parameters: ICL size, hSTS, vSTS, and LT. It did not include anterior chamber structural parameters nor did it include more ciliary sulcus structural parameters. Therefore, the interpretation of vaulting was limited.

Wu et al. [30] studied the preoperative and postoperative data of 328 cases (328 eyes) of ICL implantation and verified seven vaulting prediction formulas, including NK, KS, and Zhu. The results showed that the MedAEs of NK, KS, and Zhu formula were 141.50, 101.00, and $225.98 \mu\text{m}$, respectively. The proportions of PE within $\pm 200 \mu\text{m}$ were 68.9%, 79.9%, and 45.3%, respectively. The KS formula had the highest accuracy, whereas the Zhu formula had the lowest. The present study also showed that the Zhu formula had limited prediction accuracy (MedAE, $215.47 \mu\text{m}$), which aligned with the results of the aforementioned studies. However, the KS formula only showed advantage in APE comparison with an ICL size of 12.1 mm, with no significant difference between the two formulas for overall APE.

This study has some limitations. First, we used data from both eyes of the same patient. Although several researchers have used this method in previous studies [18, 31], such collection reduces the representativeness of the sample. We will further increase the sample size of singular eyes in subsequent studies. Second, this study included more ocular parameters than similar studies. However, owing to the complexity of the intraocular structure, the final PE in the WL formula only accounted for 81.3% in the $\pm 250 \mu\text{m}$ range, and 19.7% of the vaulting could not be explained by the formula. Therefore, new ocular parameters should be explored to improve the accuracy of this formula. Third, at present, UBM can only be used to explore the posterior chamber structure of the eye; however, the measurement of UBM is not as reproducible as that of optical instruments, such as CASIA2 AS-OCT, because of many subjective factors. To minimize manual errors, the UBM measurements in this study were conducted by a single experienced physician, ensuring consistent placement of the probe at the corneal center for axial scanning. The images were acquired when the echo arcs of both the anterior and posterior surfaces of the cornea, as well as those of the anterior and posterior surfaces of the lens, were distinctly visualized and aligned in a coherent straight line. When measuring the ciliary sulcus structure, anatomical locations, such as scleral process and iris root, were used to improve the measurement repeatability. Fourth, this study focused on the establishment of the WL formula, and the data for the model validation group were limited. We plan to expand the sample size of the validation group in a follow-up study to further demonstrate the vaulting prediction accuracy of the WL formula. Fifth, over time, the vaults of patients with low and medium vault ($\text{vault} \leq 750 \mu\text{m}$) stabilized starting from 1 week after surgery, and the vaults of the patients with high vault ($\text{vault} > 750 \mu\text{m}$) stabilized starting from 3 months after surgery [32]. Therefore, the WL formula must be optimized according to the expected vault size and time.

However, in clinical practice the ICL vault prediction formula still needs to be prioritized to ensure that most patients achieve an ideal vault in the short term after surgery. Finally, this study was conducted in 137 consecutive patients, with men accounting for 12.41% (17 cases) and women accounting for 87.59% (120 cases) of the study population. The majority of the patients were female, which may be attributed to the fact that women in China are more inclined to undergo ICL surgery to enhance their visual quality and change their image. Although the effect of sex on vault remains inconclusive, it is worth noting that the abnormal sex ratio of the study patients will affect the interpretation of the study results for the vault after ICL implantation in male patients.

Conclusions

The present study conducted a comprehensive analysis of 34 types of anterior and posterior chamber structural parameters, surpassing previous research efforts, to derive a novel formula for predicting the vault of the ICL (V4c) based on factors such as ICL size, CCT, ATA, hSTSL, vSTSL, CSR3, LD-ITC₉, and LD-ITC₆. Notably, both the complexity of the anterior and posterior chamber structures were thoroughly taken into account. The verification of the WL formula shows that its accuracy is superior to that of the KS formula (Ver. 4) and Zhu formula. The proportion of APE \leq 250 μ m of the WL formula was higher than that of the NK formula (Ver. 3). The WL formula provides a new and improved vaulting prediction formula for ICL implantation surgery and improves the safety of ICL surgery.

Abbreviations

ACA	Anterior chamber angle
ACV	Anterior chamber volume
ACW	Anterior chamber width
AL	Axial length
APE	Absolute prediction error
ATA	Angle-to-angle
CCT	Central corneal thickness
CLR	Crystalline lens rise
hSTS	Horizontal ciliary sulcus to ciliary sulcus
hSTSL	Distance between the hSTS plane and anterior crystalline lens surface
iACD	Internal anterior chamber depth
ICL	Implantable collamer lens
Kf	Flat keratometry
Ks	Steep keratometry
LT	Lens thickness
MedAE	Median of absolute error
PE	Prediction error
SE	Spherical equivalent
VIF	Variance inflation factor
vSTS	Vertical sulcus to ciliary sulcus
vSTSL	Distance between the vSTS plane and anterior crystalline lens surface
WTW	White-to-white

Acknowledgements

Thanks to Jingjing Wang of Shanxi Eye Hospital for the guidance of data statistics. We would like to thank Editage (www.editage.cn) for English language editing.

Author contributions

WW: Conceptualization, Data curation, Writing-original draft, Writing-review & editing. JiL: Performed ICL surgery, Writing review & editing, Methodology. LZ: Examined patients before and after surgery, Data curation, Validation, Review & editing. WL: Data curation, Formal analysis, Investigation. YC: Data curation, Article layout, Validation, Writing-review & editing, Investigation. LY: Data curation, Validation, Review & editing. ZF: Data curation, Software analysis. BW: Examined patients before and after surgery, Data curation. FC: Data curation, Data analysis, Statistical chart production. JM: Data curation, Writing-review & editing. Jul: Conceptualization, Project administration, Supervision, Writing-original draft, Writing-review & editing, Methodology.

Funding

The authors declare that financial support was received for the research, authorship, and/or publication of this article. This research was funded by the Health Commission of Shanxi Province (2021097). The funder had no role in the study, data analysis, manuscript writing, or publication.

Data availability

The datasets used and/or analyzed during the current study are available from the corresponding author on reasonable request.

Declarations

Ethics approval and consent to participate

The present study was granted ethical approval by the Ophthalmology Ethical Committee of Shanxi Province, with the reference number SXYYLL-20210601. All participants received comprehensive information regarding the study's objectives and associated risks and provided their written informed consent by signing a surgical consent form.

Consent for publication

Not applicable.

Competing interests

The authors declare no competing interests.

Author details

¹Shanxi Eye Hospital Affiliated to Shanxi Medical University, Taiyuan, Shanxi, China

²Ruiz Department of Ophthalmology and Visual Science, McGovern Medical School, University of Texas Health Science Center, Houston, TX, USA

Received: 18 June 2024 / Accepted: 2 August 2024

Published online: 16 August 2024

References

- Holden BA, Fricke TR, Wilson DA, Jong M, Naidoo KS, Sankaridurg P, et al. Global prevalence of myopia and high myopia and temporal trends from 2000 through 2050. *Ophthalmology*. 2016;123:1036–42.
- Fernández-Vega-Cueto L, Lisa C, Esteve-Taboada JJ, Montés-Micó R, Alfonso JF. Implantable collamer lens with central hole: 3-year follow-up. *Clin Ophthalmol*. 2018;12:2015–29.
- Wei R, Li M, Aruma A, Knorz MC, Yang D, Yu Y, et al. Factors leading to realignment or exchange after implantable collamer lens implantation in 10 258 eyes. *J Cataract Refract Surg*. 2022;48:1190–6.
- Liu HT, Zhou Z, Luo WQ, He WJ, Agbedia O, Wang JX, et al. Comparison of optical quality after implantable collamer lens implantation and wavefront-guided laser in situ keratomileusis. *Int J Ophthalmol*. 2018;11:656–61.
- Miao H, Chen X, Tian M, Chen Y, Wang X, Zhou X. Refractive outcomes and optical quality after implantation of posterior chamber phakic implantable collamer lens with a central hole (ICL V4c). *BMC Ophthalmol*. 2018;18:141.

6. Gjerdrum B, Gundersen KG, Lundmark PO, Potvin R, Aakre BM. Prevalence of signs and symptoms of dry eye disease 5 to 15 after refractive surgery. *Clin Ophthalmol*. 2020;14:269–79.
7. Brar S, Gautam M, Sute SS, Pereira S, Ganesh S. Visual and refractive outcomes with the Eyecryl phakic toric IOL versus the visian toric implantable collamer lens: results of a 2-year prospective comparative study. *J Refract Surg*. 2021;37:7–15.
8. Awadein H. ICL versus Veriflex. ICL versus Veriflex phakic IOL for treatment of moderately high myopia: randomized paired-eye comparison. *J Refract Surg*. 2013;29:445–52.
9. Thompson V, Cummings AB, Wang X. Implantable collamer lens procedure planning: a review of global approaches. *Clin Ophthalmol*. 2024;18:1033–43.
10. Stopyra W, Langenbacher A, Grzybowski A. Intraocular lens power calculation formulas-A systematic review. *Ophthalmol Ther*. 2023;12:2881–902.
11. Li B, Chen X, Cheng M, Lei Y, Jiang Y, Xu Y, et al. Long-term vault changes in different levels and factors affecting vault change after implantation of implantable collamer lens with a central hole. *Ophthalmol Ther*. 2023;12:251–61.
12. Zhang H, Gong R, Zhang X, Deng Y. Analysis of perioperative problems related to intraocular implantable collamer lens (ICL) implantation. *Int Ophthalmol*. 2022;42:3625–41.
13. Gimbel HV, LeClair BM, Jabo B, Marzouk H. Incidence of implantable collamer lens-induced cataract. *Can J Ophthalmol*. 2018;53:518–22.
14. Fernandes P, González-Méijome JM, Madrid-Costa D, Ferrer-Blasco T, Jorge J, Montés-Micó R. Implantable collamer posterior chamber intraocular lenses: a review of potential complications. *J Refract Surg*. 2011;27:765–76.
15. Tang C, Sun T, Duan H, Liu Y, Qi H. Evaluation of the performance of two nomograms and four vault prediction formulas for implantable collamer lens size selection. *J Refract Surg*. 2023;39:456–61.
16. Chen X, Ye Y, Yao H, Liu C, He A, Hou X, et al. Predicting post-operative vault and optimal implantable collamer lens size using machine learning based on various ophthalmic device combinations. *Biomed Eng Online*. 2023;22:59.
17. Zhu QJ, Chen WJ, Zhu WJ, Xiao HX, Zhu MH, Ma L, et al. Short-term changes in and preoperative factors affecting vaulting after posterior chamber phakic Implantable Collamer Lens implantation. *BMC Ophthalmol*. 2021;21:199.
18. Wu H, Zhong DJ, Luo DQ, Zhang LY, Liu J, Wang H. Improvement in the ideal range of vault after implantable collamer lens implantation: a new vault prediction formula. *Front Med (Lausanne)*. 2023;10:1132102.
19. Zhang X, Chen X, Wang X, Yuan F, Zhou X. Analysis of intraocular positions of posterior implantable collamer lens by full-scale ultrasound biomicroscopy. *BMC Ophthalmol*. 2018;18:114.
20. Oleszko A, Marek J, Muzyka-Wozniak M. Application of a partial least squares regression algorithm for posterior chamber phakic intraocular lens sizing and postoperative vault prediction. *J Refract Surg*. 2020;36:606–12.
21. Trancón AS, Manito SC, Sierra OT, Baptista AM, Serra PM. Determining vault size in implantable collamer lenses: preoperative anatomy and lens parameters. *J Cataract Refract Surg*. 2020;46:728–36.
22. Kim T, Kim SJ, Lee BY, Cho HJ, Sa BG, Ryu IH, et al. Development of an implantable collamer lens sizing model: a retrospective study using ANTERION swept-source optical coherence tomography and a literature review. *BMC Ophthalmol*. 2023;23:59.
23. Di Y, Li Y, Luo Y. Prediction of implantable collamer lens vault based on preoperative biometric factors and lens parameters. *J Refract Surg*. 2023;39:332–9.
24. Wei R, Cheng M, Niu L, Wang L, Luo X, Li M, et al. Outcomes of the EVO ICL using a customized non-horizontal or horizontal implanting orientation based on UBM measurement: a pilot study. *Ophthalmol Ther*. 2022;11:1187–98.
25. Zheng QY, Xu W, Liang GL, Wu J, Shi JT. Preoperative biometric parameters predict the vault after ICL implantation: a retrospective clinical study. *Ophthalmic Res*. 2016;56:215–21.
26. Zhang P, Guo C, Wang S, Jiang W, Wang D, Yan H. Influencing factors comparing different vault groups after phakic implantable collamer lens implantation: review and meta-analysis. *BMC Ophthalmol*. 2024;24:70.
27. Zou Q, Zhao S, Cheng L, Song C, Yuan P, Zhu R. Effects of crystalline lens rise and anterior chamber parameters on vault after implantable collamer lens placement. *PLoS ONE*. 2024;19:e0296811.
28. Igarashi A, Shimizu K, Kato S, Kamiya K. Predictability of the vault after posterior chamber phakic intraocular lens implantation using anterior segment optical coherence tomography. *J Cataract Refract Surg*. 2019;45:1099–104.
29. Nakamura T, Isogai N, Kojima T, Yoshida Y, Sugiyama Y. Optimization of implantable collamer lens sizing based on swept-source anterior segment optical coherence tomography. *J Cataract Refract Surg*. 2020;46:742–8.
30. Wu H, Luo DQ, Chen J, Wang H, Zhong DJ. Comparison of the accuracy of seven vault prediction formulae for implantable collamer lens implantation. *Ophthalmol Ther*. 2024;13:237–49.
31. Ando W, Kamiya K, Hayakawa H, Takahashi M, Shoji N. Comparison of phakic intraocular lens vault using conventional nomogram and prediction formulas. *J Clin Med*. 2020;9:4090.
32. Kojima T, Maeda M, Yoshida Y, Ito M, Nakamura T, Hara S, et al. Posterior chamber phakic implantable collamer lens: changes in vault during 1 year. *J Refract Surg*. 2010;26:327–32.

Publisher's Note

Springer Nature remains neutral with regard to jurisdictional claims in published maps and institutional affiliations.